ANALYSIS OF AN AUTOMOTIVE THERMOELECTRIC GENERATOR ON A GASOLINE ENGINE

by

Ilker TEMIZER*, Tahsin YUKSEL, Ibrahim CAN, and Dogan Engin ALNAK

Technology Faculty Automotive Engineering Department, Sivas Cumhuriyet University, Sivas, Turkey

Original scientific paper
https://doi.org/10.2298/TSCI180105096T

This study determined the heat, flow, and electrical power values of and automotive thermoelectric generation system integrated in the exhaust system of an internal combustion gasoline engine. The combustion analyses of the engine integrated with and without automotive thermoelectric generation were carried out. The 20 thermoelectric modules were placed on the rectangular structure which was made of the aluminum 6061 material. The thermoelectric modules were electrically connected to each other in series. The gasoline engine was operated at full load at 1250, 1750, and 2250 rpm, and the electrical energy generated by the automotive thermoelectric generation system was calculated. At the same time, the heat and flow analyses of the automotive thermoelectric generation system were performed using the ANSYS FLUENT commercial software.

Key words: *thermoelectric, internal combustion engine, CFD, heat transfer*

Introduction

Thermoelectrics is a science that examines the electrical potential that is created by the temperature differences in liquid or solid materials. Thermoelectrical system turn heat energy into electrical energy or electrical energy into heat energy. Waste heat recovery has become one of the important ways in internal combustion engines (ICE) for energy saving. It is well known that the characteristic of combustion has an important effect on engine efficiency and waste heat recycling system [1, 2]. The heat created by exhaust gases has an important potential [3]. For this reason, studies in the field of recovery of waste energy gain importance. Recently, thermoelectrics has become an important research topic. Recovery of wasted heat and conversion of it into useful energy such as electrical energy may increase the efficiency of energy conversion system and reduce demand on fossil fuels and natural resources [4-6]. Thermoelectric devices may be used for cooling, heating, power generation and sensing. The effects of thermoelectric modules (TEM) on cooling capacity was analysed to be used with the finite element method of TEM, fig. 1. Cooling power, electrical power, and performance parameters were calculated [7]. In another study, it was possible to analyse the calculations on thermoelectric devices using the finite element method [8]. A simulation study created a thermoelectric generation (TEG) system that consisted of 32 double legs. Three different filling thickness values were used as 100, 500, and 1000 mm to analyze the effects of TEG geometry. Cubic and strays of the TEG modules were chosen as 2 mm. Different temperatures were determined for

* Corresponding author, e-mail: dealnak@cumhuriyet.edu.tr

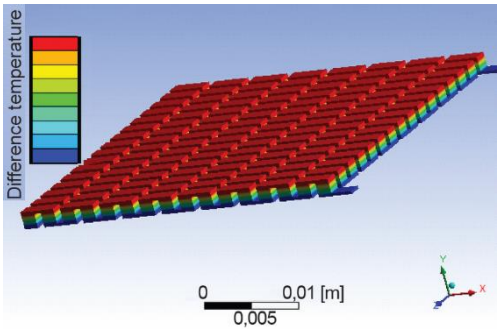

Figure 1. Thermoelectric modules (*for color image see journal web site*)

usage as 100, 300, and 500 °C. When the results of the experiment were examined, the temperature distribution was not uniform [9]. The TEG made use of the Seebeck effect in semiconductors for the direct conversion of heat into electrical energy. The electrons in the *n*-type materials that have the ability to move in semiconductors and metals serve as the holler of the *p*-type materials loading the carrier. These are alloys like Bi_2Te_3, PbTe, SiGe, and BiSb. The Bi_2Te_3 is the most preferable alloy because of its appropriate working heat and thermoelectric performance. The Seebeck coefficients of *p*-type and *n*-type materials are functions of temperature. These semiconductors are placed between two ceramic layers. Thus, thermal conductivity, electrical insulation and mechanical strength could be provided [10, 11]. Some car companies have proven their interest in exhaust heat recovery, developing system that make use of TEG. Kim *et al.* [12] designed an exhaust heat recovery system using both TEG and heat pipes. In their study, they generated a maximum of 350 W using 112 TEG. Liu *et al.* [13] investigated a thermoelectric energy generation system in which the maximum electrical power output was 183.24 W. The semiconductor material used in the fabrication of the pellets was selected according to the position of the TEG in the exhaust system. Another important issue is the temperature of the cooling water. High temperature gases passing along the exhaust pipe may be used to heat the *hot side* of the TEG while the *cold side* is created using pipes filled with water. Moreover, the cold side of the TEM may cooled by a refrigerant or air. The preliminary work focused on the design optimization of TEG system [14-18].

Experimental set-up

A prototype that works in accordance with the working principles of TEG was applied to an internal combustion gasoline engine's exhaust system. Two different fluids were used in the system to create different temperatures that are the working conditions for TEM. One of these was the exhaust gases used to create a hot surface. In this study, two different fluids were used as exhaust gases and cooling water. The 20 TEM which were connected to each other in series were placed on a rectangular structure with an aluminum alloy material. The TEM were used between the exhaust pipe and the water-cooling unit. The aluminum plate that was cut in the dimensions of 340 × 100 × 2 mm was turned into a rectangular structure in a special bending machine to achieve an angle of 90°. The dimensions of the automotive TEG (ATEG) system are given in tab. 1.

Table 1. The dimensions of ATEG

System components	Dimensions
Nozzle	L: 120 mm, D_1: 45 mm, H: 100 mm, T: 2 mm
Rectangular channel	L: 340 mm, H: 100 mm, W: 185 mm, T: 2 mm
Cooling channel	L: 340 mm, H: 35 mm, W: 185 mm, T: 15 mm, D_2: 20 mm
TEM	56 mm × 56 mm × 5 mm

In total, 20 TEM were connected to each other as 10 pieces on each surface in the experiments. The system consisted of the TEM, the inlet and outlet pipes of the exhaust gases and the water inlet and outlet. The waste heat recovery system that is shown in fig. 2 was designed for use with the exhaust pipe of the engine. This study examined the effects of an internal combustion gasoline engine that was operated at different speeds on the ATEG system. One of the most important issues was the design of the ATEG system as the design of the system directly affects the efficiency of ATEG system. From this point, the important aspects in the design of the system were:

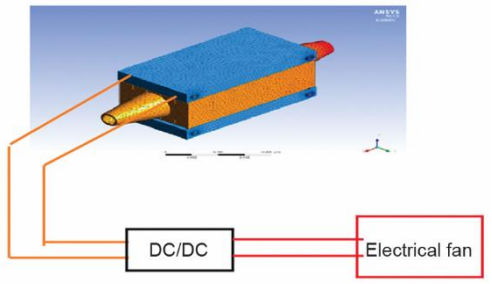

Figure 2. Thermoelectric generation (*for color image see journal web site*)

- Thermal forces need to have the ability to distribute and manage heat as comparable to a more planar design.
- The wall surface is applied to the cold side to ensure thermal conductivity, electrical insulation and water tightness.
- Exhaust gases have edge length that will not increase the surface and the opportunity to benefit from TEM.
- The input and output nozzles are created to ensure the entry and exit of the exhaust gas flow. This way, the risk of sudden flow contraction and expansion is prevented.

The experiments used a plate consisting of the 6061 T4 aluminum material. Material selection was planned by considering machinability characteristics, corrosion resistance, lightness, flexibility and heat transfer parameters.

The heat of exhaust gases in the rectangle channel allow creation of a hot surface in the TEM. Water was used to create the cold surface of the TEM in the system. Thermal paste was used to enhance the heat transfer and fill the micro-gaps on the surfaces of the TEM. The ATEG cooling system consisted of mains water that had a constant flow rate. The input speed of cooling water was stable at 0.9 m per second, and its temperature was 15 °C in all working conditions. The DC-DC converter was between the ATEG and the electrical fan as an electrical circuit. The DC-DC converter under with the brand of mean well with the number of SD-1000L-12 providing charge to the electrical fan in a certain voltage was used to prevent electrical fluctuations and transfer electrical power. Then, electrical power was generated with the temperature difference between the two sides of the TEM. A thermocouple K-type was used in the heat measurements. The electrical current generated by the modules was measured with a multimeter. The test set comprised a Baturalp Taylan brand engine dynamometer (test cell) bench and Loncin-brand gasoline engine with one cylinder and four-strokes. Electrical dynamometers that controlled the speed and load values of the gasoline engine were connected to determine the performance of the ATEG system placed behind of the muffler on the exhaust system. The engine was operated at 1250, 1750, and 2250 rpm under full throttle and load.

Electrical dynamometers are used as loading units [Nm] in engines. The testing set that was used in the workshop of Automotive Engineering Department of Technology Faculty in Cumhuriyet University is schematically shown in fig. 3. The objective was to determine the effects of the engine on the TEM. The output and input temperatures of the exhaust gases were recorded by measuring the TEM top and bottom surface temperatures and voltage and current

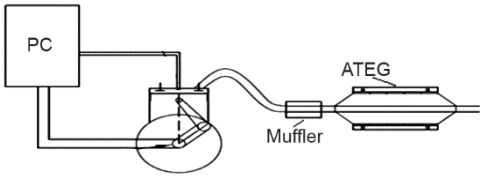

Figure 3. Testing set

Table 2. The characteristics of the engine that was used in the experiments

Engine	Loncin G420 F
Engine cooling technology	Air cooling
Number of cylinders	1
Cylinder volume	420 cc
Maximum power	3600 rpm, 8.5 kW
Compression ratio	8.3:1

values. The characteristics of the internal combustion gasoline engine connected to the test stand are given in tab. 2.

The engine was operated at different speeds under full load. The numerical calculations were made in 3-D independent from time. The ANSYS FLUENT program was used for CFD. For CFD, the definition of the solution zone geometry was first described, the solution zone was then divided into sub-elements, and the grid was formed. The flow properties were defined, and the boundary conditions on the elements were determined. The finite volume method uses a control-volume-based technique to transform conservation equations into numerically solvable system of algebraic equations. This technique involves obtaining the discrete equations that provide the control volume for the variables as a result of taking the integration of conservation equations for each control volume. With the iterative solution of system of linear equations obtained by linearization of discrete equations, variables such as velocity, pressure and temperature are updated until they provide the given convergence measure. For the optimum network structure to be prepared, a tighter network structure was created, and the most appropriate network type was selected in the critical flow regions where the speed, pressure and temperature changes were large. For this reason, especially in the cavities, sections with the tightest network structure were formed, and the looser network structure was preferred in the other regions. The number of network elements was taken as 1219250. Exhaust gas and water were accepted as fluids, and different temperatures were taken at different speeds. Aluminum was selected as the material. The results were obtained for seven different engine speeds. A stable regime and a k-ε turbulent flow model were chosen in the calculations. Considering the no-slip condition in the upper and lower walls, the boundary conditions were taken in the walls as: $u = v = w = 0$; at the channel input as: u_{cf}, T_{cf} and at the channel output as: P_{cf}. The working area consisted of an inlet zone on the inlet side of the exhaust duct and a circular cross-section inlet with a diameter of 45 mm. The flow rate and temperature of the fluid that went into the channel varied depending on the engine's speed. We had two separate inlet and outlet zones at the top and bottom of the channel, a fluid (water) with an average temperature of 15 °C enters this area and leaves the area from the outlet of the channel in the upper zone.

Equations involving viscous, heat transfer, non-reactive, incompressible, 3-D and non-perpetual flow were the equations of conservation of mass, eq. (1), conservation of momentum, eq. (2), which is Newton's second law, and energy conservation, which is the first law of thermodynamics, eq. (4).

Continuity equation:

$$\frac{\partial \rho}{\partial t} + \frac{\partial (\rho u_k)}{\partial x_k} = 0 \tag{1}$$

Navier-Stokes equation:

$$\frac{\partial(\rho u_i)}{\partial t}+\frac{\partial(\rho u_i u_k)}{\partial x_k}=-\frac{\partial p}{\partial x_i}+\frac{1}{\mathrm{Re}}\frac{\partial \tau_{il}}{\partial x_j} \tag{2}$$

where τ_{ij} is the viscous tensile tensor and is as in eq. (3):

$$\tau_{ij}=\mu\left(\frac{\partial u_i}{\partial x_j}+\frac{\partial u_j}{\partial x_i}\right)-\frac{2}{3}\mu\frac{\partial u_k}{\partial x_k}\delta_{ij} \tag{3}$$

This expression shows the conservation of the three components of momentum. The expression on the left side shows the momentum change in the unit volume, and the one on the right side shows the viscous and pressure forces acting on the flow channel. In addition to these equations, because the heat transfer in the flow was also examined, the conservation of energy equation was also used:

$$c_v\frac{\rho T}{\partial t}+c_v\frac{\rho u_k T}{\partial x_k}=\frac{\gamma}{\mathrm{Re}\,\mathrm{Pr}\,\partial x_k}\left(k\frac{\partial T}{\partial x_k}\right)-(\gamma-1)p\frac{\partial u_k}{\partial x_k}+\frac{\lambda-1}{\mathrm{Re}}\Phi \tag{4}$$

Results and discussion

Experimental results

The experimental section presents a description of the experimental set-up and testing method to validate the newly proposed idea. The measurements were in the range of 1250, 1750, and 2250 rpm engine speeds. As shown in fig. 4, the maximum TEM surface temperature was measured as 148.9 °C in the hot surface and 43.5 °C in the cold surface when the engine ran at 2250 rpm. Due to experimental difficulties, only two different surface temperatures of the first TEM could be measured. In the study, the temperature measurements were recorded with the help of thermocouples placed on the surfaces of the TEM.

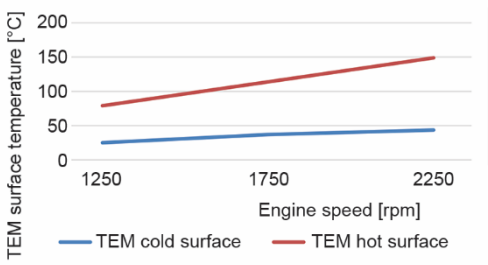

Figure 4. The temperatures on the surface of TEM

The speed and unit time of the internal combustion engines increased as the piston speed increased. Based on these increases, the exhaust gas temperature and flow rate also increased. In the experimental studies, the temperature was in proportion with the engine speed value. The increase in the speed of the engine increased both the top and bottom surface temperatures of the TEM. The temperature of the exhaust gases in the ATEG system decreased as a result of convectional heat transfer and cooling fluid-flow in the system. However, the exhaust gas temperatures in the ATEG system increased with the increase in speed. As shown in fig. 5, the increase in the amount of fuel received by the engine at unit time increased both the combustion speed and temperatures at the end of combustion. In parallel to the increase in the speed, the exhaust gases showed an increase in their speed values. Figure 6 shows the flow rate of the exhaust gases measured at the ATEG inlet.

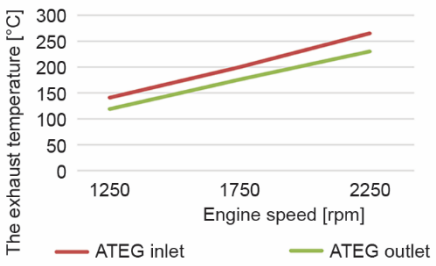

Figure 5. The temperatures of exhaust gases

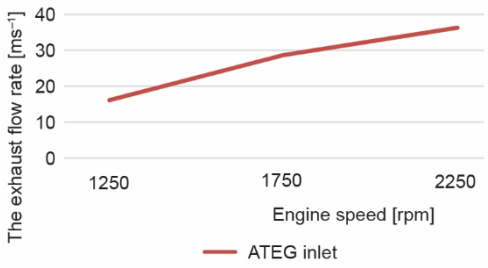

Figure 6. The flow rates of exhaust gas

Table 3. The electrical results for different engine speeds and loads

Engine speed [rpm]	Voltage [V]	Current [A]	Electrical power [W]
1250	6.04	1.22	7.36
1750	11.96	1.8	21.52
2250	16.4	2	32.8

The maximum circuit voltage in the ATEG system that transformed the waste heat energy into electrical energy was recorded as 16.4 V for 20 TEM. As shown in tab. 3, when the engine speed increased, the value of the produced electrical energy increased. However, this increase was not a linear one. The voltage values that were obtained were outside the regular operational voltage interval of the DC/DC converter. These measurements were measured between the ATEG system and the DC/DC converter. The converter drew a certain electrical voltage and current, but it could not transfer these to the receiver at the fixed output voltage of 12 V. Selection of different voltage intervals for the received led the converter to draw some amount of current.

Heat and flow analysis results

In the ANSYS fluent software, the experimental data that were obtained as a result of the engine operating at different values of speeds were determined as the boundary conditions. The results of the analysis showed the speed and temperature distributions in the ATEG system, fig. 7. The boundary conditions were updated for each analysis under different operating conditions in the engine. The temperatures found in the numerical calculations were somewhat higher in comparison to the experimental results. Since the losses that occur in real operating conditions were neglected during the analysis, we found that the emergence of a temperature difference was a normal result in the experimental and numerical studies. The cooling system of the ATEG system was effective in cooling the exhaust gases at all three axes. When the temperature analyses were examined, experimentally measured output temperatures showed similarities with analysis results.

When the speed analyses were examined, the exhaust flow rate increased in the inlet and outlet regions at all operating conditions, and the speed decreased with the expansion of the section in the middle regions, fig. 8. When we look at these results, the sectional structure of the inlet and outlet regions created a jet effect. Then, in the direction of flow velocity, the velocity gradually decreased in the exhaust channel. This reduction and fins improved the heat transfer in this region. At the same time, it is possible to say that, due to gravitational acceleration, the flow velocity accelerated downward, *i. e.*, in the direction of z. In future work, it may be possible to improve heat transfer with flow breakers which may be placed in the channel.

The size of the flow area may affect the flow structure. This creates a pressure effect on the engine in the opposite direction, causing the performance of the engine to decrease. For

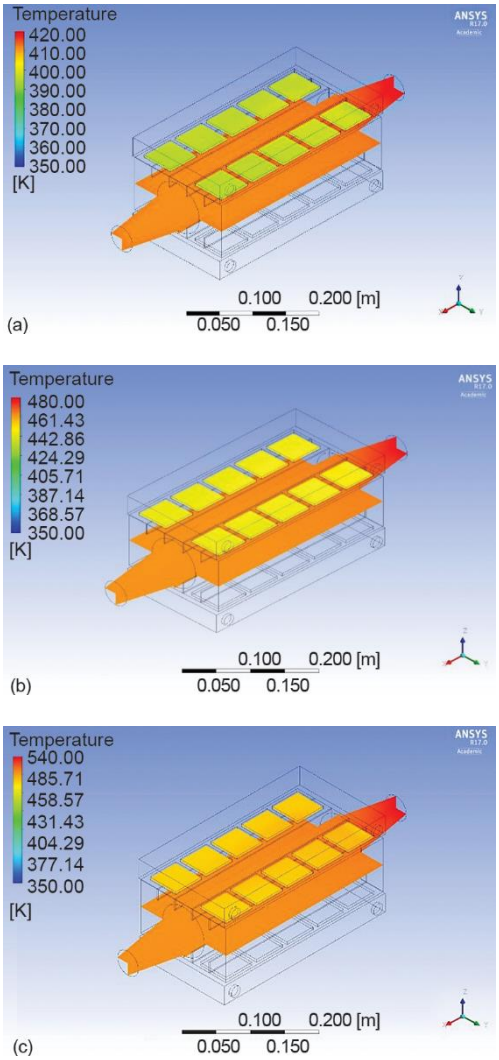

Figure 7. The temperature distribution of the ATEG system at 1250 rpm (a), 1750 rpm (b), and 2250 rpm (c) (*for color image see journal web site*)

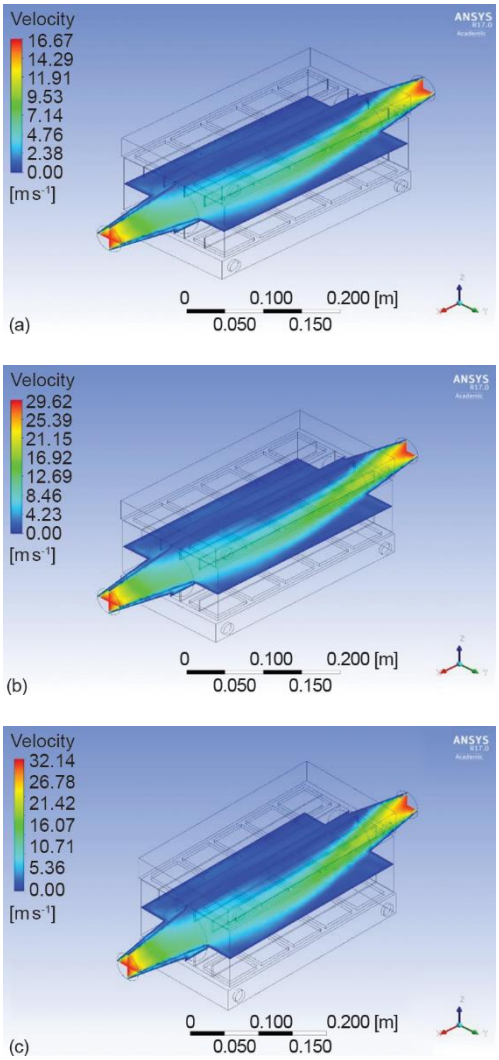

Figure 8. The exhaust flow rate in the ATEG system for 1250 rpm (a), 1750 rpm (b), and 2250 rpm (c) (*for color image see journal web site*)

this reason, choosing as large a geometry as possible may be the wrong method. For all the analysis results, it is seen that, depending on the shape factor, the speed first decreased in the corners, then gradually increased again in the flow direction. The pressure loss coefficient increased in parallel with the increase in engine speed. As a result of this phenomenon, the pressure loss between the inlet and outlet of the ATEG increased. As it may be seen in figs. 9 and 10, the increase in pressure loss between 1250 rpm and 1750 rpm was low. In particular, it was greater at 1750 rpm and 2250 rpm. This result was proportional to the flow rate of the exhaust gas. At the same time, contraction, expansion, fins, surface frictions were the main causes of this loss.

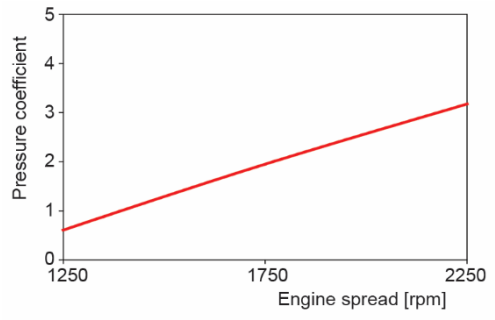

Figure 9. The pressure loss coefficient at different engine speeds

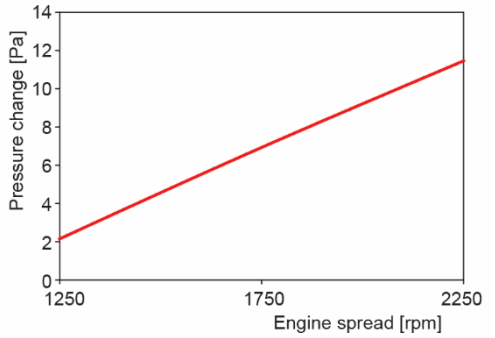

Figure 10. The pressure change at different engine speeds

Conclusion

Electrical energy was produced in parallel to increase in engine speeds. A total of 20 TEM were used in the ATEG system. The maximum electrical power that was produced was calculated as 32.8 W. Moreover, 3-D heat and flow analyses of the ATEG system were performed.

The results were compared with the experimental results using ANSYS package program and it was found to be compatible with the experimental results. In the ANSYS package program, results were obtained at different engine speeds (1250-2250 rpm). As a result, the maximum speed of 16.67 m/s and 37.49 m/s was reached in the ATEG system. The maximum temperature values are between 420 °C and 540 °C. It is recommended that different models be made in the following studies and these models should be done in ANSYS package program.

This study proved which alternator could be the alternative energy source in supplying electrical energy for internal combustion engines.

Acknowledgment

Authors thank Cumhuriyet University Scientific Research Fund for their valuable financial support with the project number TEKNO-004.

Nomenclature

c_P – constant pressure specific heat, [Jkg^{-1}K^{-1}]
h – heat transfer coefficient, [Wm^{-2}K^{-1}]
k – thermal conductivity, [Wm^{-1}K^{-1}]
Nu – Nusselt number (= hL/k)
x, y, z – co-ordinates
u, v, w – velocities in x-, y- and z-directions, [ms^{-1}]
L – length, [mm]
H – height, [mm]
W – width, [mm]
T – thickness, [mm]
D_1 – shrinkable cross-sectional diameter, [mm]
D_2 – water inlet and outlet diameter, [mm]

Greek symbols

μ – dynamic viscosity, [kgm^{-1}s^{-1}]
ν – kinematic viscosity, [m^{2}s^{-1}]
ρ – density, [kgm^{-3}]

Abbreviations

TEM – thermoelectric module
TEG – thermoelectric generation
ATEG – automotive thermoelectric generation

References

[1] Balci, C., Climatization of a Vehicle Cabinet by an NH_3-H_2O Absorption System Performing with Exhaust Gas Energy, postgraduate thesis, Suleyman Demirel University, Isparta, Turkey, 2011

[2] Temizer I., *et al.*, Effects on Vehicle System of Technology Thermoelectric, *Batman University Journal of Life Sciences, 1* (2012), 2, pp. 199-209
[3] Goncalves, L. M., *et al*., Heat-Pipe Assisted Thermoelectric Generators for Exhaust Gas Applications, *Proceedings*, ASME 2010 International Mechanical Engineering Congress and Exposition. Volume 5: Energy Systems Analysis, Thermodynamics and Sustainability; NanoEngineering for Energy; Engineering to Address Climate Change, Parts A and B. Vancouver, British Columbia, Canada, 2010, pp. 1387-1396
[4] Saqr, K. M., *et al.*, Thermal Design of Automobile Exhaust Based Thermoelectric Generators: Objectives and Challenges, *International Journal Automotiv Technology, 9* (2008), 2, pp. 155-160
[5] Thacher, E. F., *et al*., Progress in Thermoelectrical Energy Recovery from a Light Truck Exhaust, paper presentation at the DEER conf., https://www.energy.gov/eere/office-energy-efficiency-renewable-energy
[6] Thacher, E. F., *et al.*, Testing of an Automobile Exhaust Thermoelectric Generator in a Light Truck, *Automobile Engineering, 221* (2007), 1, pp. 95-107
[7] Antonova, E. E., Looman, C. D., Finite Elements for Thermoelectric Device Analysis in ANSYS, *Proceedings*, ICT 2005, 24th International Conference on Thermoelectrics, Clemson, S. C., USA, 2005, pp. 215-218
[8] Li, S. L., *et al.*, Thermo-Mechanical Analysis of Thermoelectric Modules, *Proceedings*, Microsystem Packaging Assembly and Circuits Technology Conference, 2010, pp. 1-4
[9] Admasu, T. B., *et al.*, Effects of Temperature Non-Uniformity over the Heat Spreader on the Outputs of Thermoelectric Power Generation System, *Energy Conversion and Management, 76* (2013), Dec., pp. 553-540
[10] Hsu, T. C., *et al.*, An Effective Seebeck Coefficient Obtained by Experimental Results of a Thermoelectric Generator Module, *Applied Energy, 88* (2011), 12, pp. 5173-5179
[11] Kulbachinskii, V. A., Kaminskii, A. Y., Thermoelectric Power and Shubnikov-de Has Effect in Magnetic Impurity-Doped $B\dot{I}_2Te_3$ and $B\dot{I}_2Se$, *Journal of Magnetism and Magnetic Materials, 272* (2004), Part 3, May, pp. 1991-2015
[12] Kim, S. K., *et al.*, Power Generation System for Future Hybrid Vehicles Using Hot Exhaust Gas, *Journal of Electronic Materials, 40* (2011), 5, pp. 778-783
[13] Liu, X., *et al.*, An Energy-Harvesting System Using Thermoelectric Power Generation for Automotive Application, *Electrical Power and Energy System, 67* (2015), May, pp. 510-516
[14] Hajmohammadi, M. R., *et al.*, Effects of a Thick Plate on the Excess Temperature of Iso-Heat Flux Heat Sources Cooled by Laminar Forced Convection Flow: Conjugate Analysis, *Numerical Heat Transfer, Part A: Appl, 2* (2014), 2, pp. 205-216
[15] Abouzar, P., *et al.*, Investigations on the Internal Shape of Constructal Cavities Intruding a Heat Generating Body, *Thermal Science, 19* (2012), 2, pp. 164-179
[16] Najafi, H., *et al.*, Energy and Cost Optimization of a Plate and Fin Heat Exchanger Using Genetic Algorithm, *Applied Thermal Engineering, 31* (2011), 10, pp. 1839-1847
[17] Hajmohammadi, M. R., *et al.*, Improvement of Forced Convection Cooling due to the Attachment of Heat Sources to a Conducting Thick Plate, *J. Heat Transfer, 135* (2013), 12, pp. 124504-214508
[18] Kim, T. Y., *et al.*, Waste Heat Recovery of a Diesel Engine Using a Thermoelectric Generator Equipped with Customized Thermoelectric Modules, *Energy Conversion Management, 124* (2016), Sept., pp. 280-286

Paper submitted: February 20, 2018
Paper revised: November 25, 2018
Paper accepted: November 26, 2018